UCRL - 76049
PREPRINT

Conf-740992--1

LAWRENCE LIVERMORE LABORATORY
University of California / Livermore, California

EXPERIMENTAL STUDIES OF VIBRATIONLIKE NUCLEI THROUGH THEIR ELECTROMAGNETIC PROPERTIES

R.A. Meyer

September 17, 1974

This paper was prepared for submittal to
Proceedings of the Conference on Vibrational Nuclei, Zagreb, Yugoslavia
September 23-27, 1974

EXPERIMENTAL STUDIES OF VIBRATIONLIKE NUCLEI THROUGH THEIR ELECTROMAGNETIC PROPERTIES*

R. A. Meyer

Lawrence Livermore Laboratory, University of California

Livermore, California 94550

INTRODUCTION

The electromagnetic field, as well as its interaction with nuclei to produce electromagnetic radiation, is well understood.[1-4] Because of this, data on electromagnetic transitions can provide critical measurements on many aspects of nuclear structure. A study of gamma-ray transition rates allows the study of various details of the nuclear wave function. Further, it is often possible to trace a particular transition in a series of related nuclei and thereby systematically study a particular aspect of nuclear structure. Moreover, these properties and their trends can often provide a significant test of various nuclear models and allow one to suggest improvements in the models. Thus, it is better to pay attention to what features of vibrationlike nuclei have been elucidated by the study of electromagnetic radiations than to discuss the basic electromagnetic process.

A number of improvements in the description of vibrationlike nuclei have been made by the inclusion of multiparticle configurations. Several of these improvements have been suggested by experimental studies of electromagnetic

*Work performed under the auspices of the U.S. Atomic Energy Commission.

transitions in nuclei alone or in conjunction with reaction spectroscopy studies. The influence of multiparticle effects on vibrationlike nuclei can be well illustrated by a discussion of the odd-mass nuclei in the region of the nuclear chart bounded by Z of approximately 50 and N less than 82. Therefore, after a description of experimental techniques, we will first look at how the inclusion of three quasiparticle effects can provide a model consistent with the results of various experimental studies. These will include: the two-particle, one-hole (2p 1h) states in the odd-mass antimony nuclei; three-particle clustering in the iodine nuclei; and one-proton, two-neutron ($\pi\nu\nu$) configurations near the N = 82 shell closure. Second, we will discuss how the inclusion of the coriolis force may explain the rotationlike structure observed in spectroscopy studies of the lanthanum and indium nuclei. Third, we will discuss how recent gamma-ray spectroscopy studies may explain the apparent deviation from vibrationlike character of the N = 81 nuclei. The last subject that should be mentioned is the systematics of higher-order electromagnetic processes in the tin region. In each case discussed, a short description of the deviation from simple vibrationlike character will be followed by a specific case. This will allow a detailed comparison of the various nuclear models currently available and experimental data.

EXPERIMENTAL TECHNIQUES

Often the critical test of a nuclear model involves measurement of a gamma ray that represents a transition far less probable than others. In the past few years, the development of a number of experimental devices for

the detection of low-intensity gamma rays has allowed us to probe the nucleus further than thought possible before. A large body of data on electromagnetic transition probabilities is obtained from the measurement of gamma rays from radioactivity. Consequently, the discussion will be limited to current techniques used in the attainment of radioactive sources, their measurement, and the analysis of raw data. Where possible, I will illustrate these with equipment available at LLL.

A pure isotopic species is the most ideal radioactive source. To isolate isotopically pure sources with short half-lives from the fission process, the fission-fragment analyzer developed by P.C. Stevenson[5] is best; devices such as "Tristan and Isolde" at Ames, Iowa, U.S.A.,[6] and CERN[7] are useful for extracting gaseous fission products and spallation products, respectively. For longer-lived radioactive sources, off-line isotope separators can be used. The high yield attained by P. Johnson[8] on the LLL isotope separator has allowed the collection of up to 99% of the original isotopic radioactivity.

Prior chemical purification is necessary for sources that are to be mass spearated with off-line devices. There are numerous chemical purification techniques[9]; however, two recent developments should be mentioned. The first concerns the separation of rare earth elements. Mode and coworkers[10] have developed high-pressure resin columns in which they have attained single-element separation within 30 min to 1 hr. The second development involves separating gases by gas-chromatographic techniques. Interfacing a small computer with this technique allows the automatic separation of xenon from all other fission-product gases.[11]

A number of the critical studies to be discussed depend on the rapid isolation of a particular element from the products of thermal fission. For this, we have developed a microcomputer-controlled system that automatically controls the irradiation, delivery, and chemical separation of selected fission products. For example, we can separate antimony within 29 sec after the end of irradiation.[12] The swift separation of fission products has benefitted in the past few years by the excellent work of Prof. G. Herrmann and his coworkers at Mainz.[13]

There are numerous discussions on current gamma-ray spectroscopy techniques.[14] However, mention should be made of a key device in the measurement of very low-abundance gamma rays present in radioactive decay: the Compton Suppression Spectrometer as designed by D.C. Camp.[15] In all germanium detectors, the Compton distribution from higher energy gamma rays may mask less intense lower energy gamma rays; however, in the Compton Suppression Spectrometer, the Compton events are significantly reduced in the final spectra. This spectrometer allows detection of gamma rays tens-to-hundreds-of-thousands times less intense than higher energy gamma rays. Such a technique is particularly significant when searching for gamma rays that are forbidden by a nuclear theory or model.

Generally, gamma-gamma coincidence experiments are performed using a memory buffer with magnetic tape readout. An extension of this type of system to three parameters allows measurement of the time interval between pairs of gamma rays. This technique is useful to measure lifetimes in the range of nanoseconds to milliseconds. A more sophisticated gamma-gamma spectrometer has been developed by L.G. Mann and his coworkers at the Radiochemistry Division of LLL.[16] This megachannel system utilizes a small computer-based

coincidence spectrometer with a disc memory. Such a device permits on-line analysis of coincidence data.

Measurement of conversion electrons is most readily made with Si(Li) detector systems. However, this technique is limited by the fact that Si(Li) detectors are very sensitive to the Compton process, and, hence, produce large backgrounds. To overcome such a difficulty, we have developed a unique instrument incorporating a magnetic field that bends the electrons in a trochoidal path, focusing them on a silicon detector shielded from the source and its gamma rays.

The analysis of raw gamma-ray spectroscopy data involves the reduction of multichannel spectra. The computer code GAMMANL has been developed by R. Gunnink and coworkers[17] for use on the LLL CDC7600* and other types of computers.[18] This technique utilizes a realistic sigmodial background for photopeaks and fits the photopeak shape with a skewed gaussian.[17] The program SAMPO is superior for reducing conversion-electron spectra, particularly when used in the VISTA interactive mode.[19] A newer integrated concept combines a small disc computer system with a gamma-ray spectrometer system and modified GAMMANL routine.[20]

TWO-PARTICLE, ONE-HOLE STATES

The low-energy-level structure systematics for the odd-mass antimony (Z = 51) nuclei are shown in Fig. 1, where the insert shows the rapid decrease

*Reference to a company or product name does not imply approval or recommendation of the product by the University of California or the U.S. Atomic Energy Commission to the exclusion of others that may be suitable.

in energy for all levels with respect to the $g_{7/2}$ orbital as the neutron number decreases.[21-23] A simple weak-coupling model of single particle and single particle plus phonon cannot adequately account for all of the levels observed below the pairing gap in these nuclei. However, reaction-spectroscopy studies have suggested that the excess states have strong two-particle, one-hole character (2p 1h).[24] Recently Vanden Berghe and Degrieck[25] have attempted to calculate the structure of the antimony nuclei, taking into account the 2p-1h states and their interaction with the single-particle and phonon-coupled states.

The ^{121}Sb nucleus is an ideal case to study the nature of high-spin, positive-parity levels, for both 2p-1h and particle-phonon levels occur within a few hundred keV of each other, and these levels are populated by beta decay, as well as by Coulomb-excitation techniques. Thus any theoretical calculation is put to a stringent test, for it must not only properly predict the proximity of these levels, but also yield the measured transition moments [B(E2)↓ in particular].

The results of recent gamma-ray spectroscopy studies[26,27] are shown in Fig. 2. The $11/2^+$ level and all four high-spin levels observed in excitation studies are populated in the beta decay of ^{121}Te^m. Also, the branching ratios for the decay of the three $9/2^+$ levels are quite distinct from each other. The 1035-keV level has only seven parts per thousand populating the ground state, while the 1145-keV level decays 73% and the 947-keV level decays 10% of the time to the $5/2^+$ ground state.

The calculations of Vanden Berghe and Degrieck[25] predict all three $9/2^+$, the $7/2^+$, and the $11/2^+$ levels at approximately 1 MeV. The branching ratios

from the three $9/2^+$ levels to the ground and first excited states are consistent with their wave functions. The near lack of branching of the 1035-keV level to the $5/2^+$ ground state is understood in terms of a very small $|d_{5/2}\ 12>$ component,* while the preference of decay to the ground state for the 1145-keV level comes from the dominance of the $|d_{5/2}\ 12>$ configuration.[25] A more stringent test of predicting the electric quadrupole transitions is also moderately successful. The experimental vs calculated B(E2)↓ values are given in italics on the appropriate transition in Fig. 2.[28-32]

The electromagnetic deexcitation of the $1/2^-$ and $3/2^-$ 2p-1h levels can be studied in the beta decay of ^{119}Te. The deexcitation of the $1/2^-$ and $3/2^-$ levels that have been identified in ^{119}Sb[33] are shown in Fig. 3. These are results of gamma-ray spectroscopy studies performed on ^{119}Te activity made by the ^{120}Te(γ,n)^{119}Te^{m+g} reaction at the LLL electron linac.[34,35] Although no lifetime measurements are available, the relative decay rates are consistent with the predictions of Vanden Berghe and Degrieck.[25] The apparent hindrance of the M1 transition between the two negative-parity levels is explained by a cancellation of the 2p-1h matrix elements that provide the only allowed transitions between these two levels. For the decay of the $1/2^-$ level, an E3 rate of one single-particle unit (SPU) is consistent with E3 transitions in this region of the nuclear chart.

THREE-PARTICLE EFFECTS

For the structure of iodine nuclei, the simple particle-vibration model used by Kisslinger and Sorenson[36,37] failed on several points. First, it did

*$|j\ NJ>$ means the j-shell model state coupled to the N^{th} phonon of spin J.

not account for the systematic occurrence of a second low-lying $5/2^+$ level in all of the odd-mass iodine nuclei; second, it did not account for the large B(E2)↑ observed in the $5/2_1^+ \rightarrow 7/2_1^+$ transition such as that in ^{129}I reported by Bemis and Fransson[38]; third, it did not account for the large number of levels observed at an excitation energy of 1 to 3 MeV. The situation was improved when calculations based on the suggestions of Alaga, Paar, and coworkers[39-41] were undertaken. These calculations introduce the effects of three-particle clustering in nuclei such as iodine.

Almar and coworkers[42] have recently performed calculations which include three-particle clustering in the odd-mass iodine nuclei. Their predictions for the electric quadrupole transition can be compared to the recent experimental values[45-46] and are (in units of e^2 cm^4 10^{-50}):

$2J_i/2J_f$	$5_1/7_1$	$9_1/5_1$	$3_1/7_1$	$5_2/7_1$	$7_2/7_1$	$9_1/7_1$	$11_1/7_1$
Experiment	7.3	$\leq$0.4	3.5	1.6	1.1	7.8	12.2
Almar	6.7	2.6	12.9	5.3	0.24	3.8	9.7

There is close agreement in the B(E2) value for the $5/2_1^+ \rightarrow 7/2_1^+$ transition, and most other values have the correct relative magnitude. The $3/2_1 \rightarrow 7/2_1$ transition has also been measured in ^{125}I and ^{127}I, where the values are 14.4 and 11.2 e^2 cm^4 10^{-50}, respectively,[47] and are more in agreement with theoretical predictions.

The level structure of ^{129}I from a few hundred to 1500 keV is more dense than would be expected from a simple particle-vibration picture. The inclusion of three-particle clustering in the Z = 53 nuclei improves the agreement between theory and experiment. The recent decay-scheme studies of Mann et al.,[43,48,49] in conjunction with other studies,[44-47,50] have given a

fairly complete picture of the level structure of ^{129}I. A comparison of the ^{129}I level structure is shown in Fig. 4 between experimental data and two calculations, one by Almar et al.[42] and the other by Vanden Berghe.[51]

ONE-PROTON, TWO-NEUTRON CONFIGURATIONS

A large number of negative-parity states have been observed at about 2 MeV of excitation in the Z = 53 iodine nuclei. Their origin can be best understood if we first consider the even-even Z = 52 tellurium core, where 5^- and 7^- levels have been identified in ^{122}Te to ^{134}Te, as well as several N = 80 nuclei.[52] The electric dipole transition that depopulates the levels in the even-even nuclei has a hindrance of approximately 10^8 over the single-particle estimate. Such high hindrances have led to the suggestion that these levels are predominately made from the two-neutron configuration: $[2d_{3/2}\ 1h_{11/2}]$. For the odd-mass iodine nuclei, then, we should expect one-proton, two-neutron ($\pi\nu\nu$) states built on this configuration.[53]

The negative-parity levels that have been identified in ^{131}I and ^{133}I are shown in the center of Fig. 5, where the deexcitation of selected levels is shown in the outer portions[54-56]; the decay of levels in ^{133}I up to 2 MeV is shown in Fig. 6.* The decrease in energy of excitation in the odd-mass iodine nuclei is similar to that of the negative-parity levels in the even-mass tellurium-core nuclei. The appearance of the known 9-sec,

*See Appendix I for a description of the first successful work to isolate, study, and interpret the decay of $^{133}Te^m$.

$19/2^-$ isomer of ^{133}I can be understood as the $\pi\nu\nu$ level with configuration $[\pi g_{7/2}\ \nu(d_{3/2}\ h_{11/2})_{7^-}]_{19/2^-}$. The hindrance of approximately a million for the M2 deexcitation arises from the lack of any such $\pi\nu\nu$ components in the $15/2^+$ vibrational state to which the level decays. The 7^- configuration, upon which the $19/2^-$ is built, occurs at an excitation higher than the 5^- in ^{130}Te. Correspondingly, the $19/2^-$ level would be expected at an excitation energy above the $15/2^-$ level in ^{131}Te and its deexcitation could occur through an E2 transition to the $15/2^-$ level.

The deexcitation of the $15/2^-$ level at 1797 keV in ^{131}I is by a highly hindered E1 transition to the lower lying, single-particle, vibration-coupled levels and by an E2 to the single-particle $h_{11/2}$ level. The latter transition is not expected if the 1797-keV level has a pure configuration: $[\pi g_{7/2}\ \nu(d_{3/2}\ h_{11/2})_{5^-}]$. However, the apparent hindrance factor of this E2 transition is 14 and may represent a small amount of the $|h_{11/2}\ 12>$ configuration in the 1797-keV level. A similar explanation may be appropriate for the deexcitation of the $15/2^-$ level in ^{133}I.

Two possible $13/2^-$ levels in ^{133}I at 1776 and 1990 keV should be commented on. The lower energy level has deexcitation characteristics similar to the 1899-keV level in ^{131}I and may have the configuration: $[\pi d_{3/2}\ \nu(d_{3/2}\ h_{11/2})_{5^-}]$. This configuration would be expected a few hundred keV above the $[\pi g_{7/2}\ \nu(d_{3/2}\ h_{11/2})_{5^-}]$ levels and would be expected to decay predominately to the lower levels with $\pi\nu\nu$ configurations.

OCCURRENCE OF ROTATIONLIKE STRUCTURE

Another one of the deviations from vibrationlike character occurs for the nonnormal-parity $h_{11/2}$ states coupled to the core. The particle-plus-rotor

model was suggested to explain the yrast bands observed in the (HI,xnγ) reaction experiments by Leigh et al.[57-60] However, in addition to the yrast band, lower spin levels not populated in (HI,xnγ) experiments are predicted by the particle-plus-rotor model. In order of increasing energy, these include levels with j = 7/2, 9/2, 3/2, 13/2, 11/2, and 5/2. These lower spin levels provide a critical test of the particle-plus-rotor model in this region. Recently, we have given proof for the existence of the entire particle-plus-rotor band in the odd-mass lanthanum nuclei.[61-63]

The electromagnetic decay properties of the ^{133}La best serve to illustrate the decay of the rotation-aligned levels. On the top left side of Fig. 7, the levels found experimentally are compared to the results of a calculation with no free parameters by Meyer ter Vehn.[62] A more recent calculation of Meyer ter Vehn includes the effect of a Fermi energy, λ, and pairing. This provides a lowering of the levels[64,65]; as seen in the center portion of Fig. 7, a number of the levels are brought down sharply in agreement with the experimental data. The branching ratio can be calculated by first adjusting λ to the relative energy of the $9/2^-$ level with respect to the $11/2^-_1$ and then using a deformation parameter of β = 0.21 and asymmetry parameter of γ = 24° (these values are taken from the adjacent even-even nuclei ^{132}Ba and ^{134}Ce).[65] The branching ratios are:

Transition	Meyer ter Vehn	Experiment
$\frac{9/2_1 \rightarrow 11/2_1}{9/2_1 \rightarrow 7/2_1}$	~7	12
$\frac{11/2_2 \rightarrow 11/2_1}{11/2_2 \rightarrow 9/2_1}$	3.9	3.2

The lifetime of the $7/2_1 \rightarrow 11/2_1$ E2 transition is unknown; however, it should be no faster than the $2^+ \rightarrow 0^+$ E2 transition in the even-even ^{132}Ba core. Using that

value for the 249-keV transition gives a relative hindrance for the E1 transitions of 1.1×10^5, 1.4×10^6 and 6.7×10^4 for the $(7/2^- \rightarrow 5/2^+)$, $(7/2^- \rightarrow 7/2^+)$ and $(7/2^- \rightarrow 9/2^+)$ transitions.

The systematics of the low-lying levels of odd-mass lanthanum nuclei are shown in Fig. 7 (bottom). The heavy marks to the left of each level scheme indicate the energy difference between the 2_1^+ level and the ground state of the core nucleus (barium). These systematics suggest that the weak-coupling model may be applicable in explaining these positive-parity levels, at least down to ^{131}La.[66]

COEXISTENCE OF PARTICLE-CORE AND HOLE-CORE STATES

The indium nuclei also exhibit significant deviations from a simple vibrational picture. The expected single-hole and hole-vibration excitations have been identified[67,68] in the indium nuclei. The electric quadrupole strength to the hole-core states has been measured by heavy-ion Coulomb excitation and agrees with simple hole-core calculations.[67] However, early decay-scheme studies showed that many more levels than expected were present at the hole-core excitation energies,[69] having positive parity and large electric quadrupole transition moments between them.[70] Various mechanisms have been proposed to explain the occurrence of these states. Bäcklin et al.[70] have studied several of the nuclei and suggest the existence of a deformed band based on the $1/2^+[431]$ Nilsson orbital. We have considered these nuclei[71] and have suggested that calculations more in the framework of the rotation-aligned scheme would better account for these levels.[72]

In our spectroscopy studies of the odd-mass nuclei,[73-77] it has been possible to study the decay of several of the low-spin positive-parity levels. The first and second members of the positive-parity band have been observed in

beta decay of ^{111}Sn[73] and (p,xnγ) experiments.[78,79] They have been observed in ^{113}In by (p,xnγ),[78,79] and as shown in Fig. 2 (bottom), we have observed the $1/2^+$ level at 1029 keV populated in the beta decay of ^{113}Sn.[74] In the case of ^{115}In, we can identify at least two low-spin bands.[75,76] The bands are observed in ^{117}In[76,79] and ^{119}In[79] as well. In all of these, the main electromagnetic decay features are the highly hindered, electric dipole transitions to the known hole states and strong intraband M1 and E2 transitions.

The best case to discuss is ^{115}In, for it has been studied by the largest number of varied techniques. Besides the decay-scheme[70,71] and Coulomb-excitation[67,68,80,81] studies, reaction studies have also identified the hole states[82-84] of ^{115}In. The (^3He,d) reaction studies have shown strong 1p-2h strength in the ^{115}In levels that are thought to have particle-cadmium-core character.[85] Also the quadrupole moment of the lowest $3/2^+$ level has been measured by Haas and Shirley[86] as 0.60 ± 0.08b. Unfortunately, most theoretical work has been on the calculations of the hole-vibration states,[87-89] while only one attempt has been made to calculate simultaneously the hole-tin-core and particle-cadmium-core states and their possible mixing.[90]

The electromagnetic decay of the 1p-2h states is consistent with a configuration quite different from a simple hole-core picture. The E2 transition between the $1/2^+$ and $3/2^+$ levels has been shown to be collective[70] with a speed similar to the cadmium core, while the E1 transitions are hindered by factors of 10^6 to 10^7. The higher energy, low-spin, positive-parity levels decay predominately to the lower 1p-2h levels, while the E1 transitions to the known $1/2^-$ and $3/2^-$ hole states are hindered by 10^4. Recent Compton-suppression spectroscopy results[76] show that the relative

intraband E2 transition from the $9/2^+$ member of the 1p-2h band is highly favored, while the ground-state transition is hindered by at least a factor of 4000. The first $9/2^+$ hole-tin-core level lies 30 keV above the $9/2^+$ particle-cadmium-core level. Here our studies have been able to identify the E2 transitions to the two lower $5/2^+$ levels. We find that the E2 to the particle-cadmium-core state is hindered by a factor of 10 over that to the $5/2^+$ hole-cadmium level.

All of the observed properties of the 1p-2h levels in ^{115}In are consistent with a deformed configuration, and it is tempting to ascribe the 1p-2h band to a 1/2[431] Nilsson orbital. However, a more quantitative explanation should encompass an extensive coriolis calculation as a function of deformation, much in the spirit of Diamond, Stephens, and coworkers.

OTHER LOW-LYING CONFIGURATIONS

The effect of low-lying 2- and 4-proton configurations in the core can be seen in the systematics of the N = 81 nuclei shown in Fig. 8. These data come from reaction[91,92] and gamma-ray[93-98] spectroscopy studies. The three, lowest-lying levels with J^π of $3/2^+$, $1/2^+$, and $11/2^-$ have been shown to have nearly all the $d_{3/2}$, $s_{1/2}$, and $h_{11/2}$ strength, while the $g_{7/2}$ and $d_{5/2}$ strength has been shown to be fragmented over several levels.[79-81] The beta-decay studies have shown the presence of many more levels below 2 MeV in ^{133}Te[87] and ^{135}Xe[82,86] than observed in the beta decay to levels of ^{139}Ce,[83-85] ^{141}Nd,[85] and ^{143}Sm.[99] These excess levels are unaccounted for in the calculations of Heyde and coworkers,[100-103] who couple the single-neutron-hole motion to the quadrupole vibrations of the nuclear surface.

The level structure of ^{135}Xe becomes understandable when the detailed electromagnetic decay properties of the ^{135}Xe levels are considered along with the recent studies of the ^{136}Xe core.[104-106] The level structure of ^{135}Xe is shown in Fig. 9 (top) and compared to a simple ^{136}Xe experimental core-hole coupling picture. The energy and decay properties of the first three levels above 1 MeV agree well with the hole-vibration calculations of Heyde and Brussard.[100] However, some of the higher-lying levels decay in a manner consistent with the decay characteristics expected from coupling a neutron hole to the known ^{136}Xe core. An example of this is the 1968-keV $5/2^+$ level shown in Fig. 9 (bottom). Here, the E2 transition to ground state is hindered by a factor of 5×10^3 over the transition to the $7/2^+$ level at 1131 keV. Such a hindrance is consistent with the coupling of the $d_{3/2}$ ground state to the known 4_1^+ level of ^{136}Xe. Similar states are observed in ^{133}Te as is shown in Fig. 10.[12]

HIGHER-ORDER MULTIPOLARITIES

The magnetic transitions with orders higher than one are rarely observed. The M2 transitions have been reviewed by Kurath and Lawson.[107] When the M2 transition occurs between predominately single-particle levels, it is found to be hindered by a factor of 50 over simple single-particle estimates for nuclei in the tin region. An example of this is the M2 transition recently identified in the ^{125}Te nucleus.[108] Its measurement by Compton-suppression techniques allowed the assignment of the $g_{7/2}$-hole state in this nucleus.[109] The M4 transitions occur in the tin region between the low-lying $h_{11/2}$ and $d_{3/2}$ levels. The calculation of their absolute rate has been a good test of several nuclear models.[36,110]

The electric octupole transition has now been observed in a number of tin-region nuclei. These transitions are observed to compete with M2 transitions from the known $h_{11/2}$ single-particle states. Presumably the enhancement of one to two times the single-particle rate reflects the influence of the octupole state identified at about 3 MeV in many of the core nuclei.[111]

SUMMARY

The electromagnetic decay properties of odd-mass nuclei have been discussed. These data and complementary information have been used to show how multiparticle and high-j shell model states can account for the observed deviation of nuclear properties from a simple vibration-coupled picture. Of the three major effects discussed, the first was the inclusion of three quasiparticle configurations: 2p-1h configurations described the odd-mass antimony nuclei, three-particle correlations improved the description of the Z = 53 iodine nuclei, and $\pi\nu\nu$ states could account for the negative-parity levels of iodine near the N = 82 shell closure. Second, the occurrence of rotationlike bands in otherwise vibrationlike nuclei was discussed. Lastly, the levels and their electromagnetic decay properties of some N = 81 nuclei were compared to the known states in the even-even core nuclei to explain the observed deviation of the level structure from a purely vibrational picture.

In general, the descriptions of odd-mass single-particle states agree well with experimental electromagnetic transition data as seen in the top of Fig. 11. The description of quasiparticle coupling to the core vibration also gives satisfactory agreement with experimental data as seen in the middle portion of the figure. However, much work is to be done if the properties

of the rotationlike bands are to be properly calculated, as seen in the bottom of Fig. 11. A number of the somewhat artificial perturbations may be accounted for in a more natural way, though, when calculations of the type done by Struble and coworkers become available for the vibrational class of nuclei.[112]

ACKNOWLEDGMENTS

I am indebted to my coworkers in the Radiochemistry Division of the Lawrence Livermore Laboratory and elsewhere. Credit is due J.H. Landrum of LLL who developed a good deal of the fast-chemistry techniques described in these discussions. Thanks are due to Dr. Jurgen Meyer ter Vehn, who was "calculating up to the last minute" to provide the best predictions on the lanthanum data, and to Dr. G.L. Struble for discussions over this presentation. I also wish to acknowledge the support and stimulation of Dr. R.W. Hoff and Dr. C. Gatrousis.

APPENDIX I

Isolation and Spectroscopy Studies of $^{133}Te^{m+g}$ Decay

The difficulty of isolating fairly pure $^{133}Te^{m}$ from fission products for spectroscopy studies is mainly due to the fact that most techniques that isolate $^{133}Te^{m}$ also produce ^{134}Te. This latter activity in turn produces ^{134}I in equilibrium and masks the measurement of $^{133}Te^{m}$ (^{134}Te and ^{134}I have similar half-lives). The best way to isolate ^{133}Te is first to produce 2.45-min ^{133}Sb and then milk the ^{133}Te daughter. This method avoids the ^{134} because ^{134}Sb is known to have a half-life of 0.17 sec.[23] However, it has the disadvantage of requiring the handling of large amounts of fission-product radioactivity on a repetitive basis.

We have developed a microcomputer-controlled system based on an INTEL-8008, CPU-pin integrated circuit. This system allows the automatic handling of a rabbit into the reactor, irradiation, and delivery of the rabbit to one of four external stations. Once the rabbit is delivered to the fast-chemistry state, a second microcomputer takes over. This chip, which can contain up to 2000 programable steps, controls the extraction and processing of the sample. In the case of isolation of the ^{133}Te, a solution of enriched ^{235}U was irradiated in the Livermore Pool Type Reactor (LPTR) and extracted from 1 to 30 sec after entry into the LPTR core. After extraction of the solution, the antimony carrier was automatically added and the mixture dropped into hot sodium borohydride, which produced stibene gas (SbH_3). The stibene gas was then bubbled through HCl and mixed with a slurry of resin. The

slurry was dropped into a catcher and rinsed with acid. After a delay time of 2 to 3 min, the resin was washed with dilute acid to strip off the ^{133}Te that had grown in. This ended the automatic phase of the separation.

The sources were either counted for measurement of the 12.4-min ground state or stored for about 1 hr and repurified to give nearly pure $^{133}Te^{m}$. The automatic part of the separation was completed within 29 to 40 sec, and the system was ready to process a subsequent irradiation within a minimum of 90 sec.

The spectroscopy measurements used several different techniques. The singles' spectra were taken by using several Ge(Li) detector systems in succession; that is, one source was counted on detector A for one half-life. The first source was then moved to detector B and a new source was put on detector A. Repetition of this sequence with numerous sources and several detectors allowed the collection of high counting statistics for several time periods. The detectors used included large-volume Ge(Li) detectors and Ge(Li)-LEPS (low-energy photon spectrometer); the latter allowed measurement of gamma rays with energies of from 10 to 200 keV.

The gamma-gamma coincidence experiments were performed on two types of instruments. The first was the LLL megachannel analyzer. Use of this system allowed easy access to the data, for as described earlier, all data is stored on a two-million-word disk. The second gamma-gamma coincidence experiment was performed by a collaboration of LLL and University of Maryland workers at the NBS reactor. In this experiment a $^{133\text{-}134}Te$ source was produced from fission once every hour. The tellurium was adhered to a resin and the iodine daughter products were continuously eluted away by concentrated HCl. The analyses of the buffer tape gamma-gamma coincidence studies were performed on the LLL CDC-7600 computers.

REFERENCES

1. W. Heitler, The Quantum Theory of Radiation (Oxford Press, London, 1957).
2. J.M. Blatt and V.F. Weisskopf, Theoretical Nuclear Physics (J. Wiley, New York, 1953).
3. F. Weisskopf, Phys. Rev. 83, 1073 (1951).
4. S.A. Moskowski in Alpha, Beta, and Gamma Ray Spectroscopy, K. Siegbahn, Ed. (North Holland Publishing Co., Amsterdam, 1966), vol. 2, p. 863.
5. P.C. Stevenson, J.T. Larsen, and J.J. Leary, in Proc. Intern. Conf. Prop. Nuc. Far From Region Beta Stability (Leysin, 1970, CERN 70-30), vol. 1, p. 143.
6. W.L. Talbert, Jr. and J.R. McConnell, Ark. Fys. 36, 99 (1966).
7. For references on these devices see Proc. Intern. Conf. Prop. Nuc. Far From Region Stability (Leysin, 1970, CERN 70-30).
8. P. Johnson, Lawrence Livermore Laboratory, private communication (1974).
9. Radiochemical Procedures Used in the Radiochemistry Division, H. Hicks, Ed., Lawrence Livermore Laboratory (unpublished manual).
10. B.M. Morris, V.A. Mode, and D.H. Sisson, J. Chromatogr. 71, 389 (1972) and references quoted therein.
11. C.F. Smith, in Proc. Noble Gases Symp. (1973), Lawrence Livermore Laboratory, Rept. UCRL-74710.
12. R.A. Meyer, S.C. Bourret, and J.H. Landrum, Spectroscopy Studies of the Odd Mass Xe Precursors, Lawrence Livermore Laboratory, DARPA Final Rept., 1974 (in preparation).
13. G. Herrmann, University of Maine, private communication (1974). See, e.g., N. Trautmann, N. Kaffrell, H.W. Behlich, G. Herrmann, and D. Hübscher, Radiochim. Acta 18, 86 (1972).

14. See, e.g., Proc. Intern. Conf. Radioactivity Nucl. Phys., J.H. Hamilton and J.C. Manthuruthil, Eds. (Gordon and Breach, New York, 1972).

15. D.C. Camp, in Proc. Intern. Conf. Radioactivity Nucl. Phys. (Gordon and Breach, New York, 1972), p. 135.

16. J.B. Niday and L.G. Mann, in Proc. Intern. Conf. Radioactivity Nucl. Phys. (Gordon and Breach, New York, 1972), p. 313.

17. R. Gunnink and J.B. Niday, Lawrence Livermore Laboratory, Rept. UCRL-51061 (1971).

18. S.V. Jackson, University of Maryland, private communication (1974).

19. C.M. Lederer, Lawrence Berkeley Laboratory, private communication (1974).

20. R. Gunnink, J.B. Niday, and P.D. Siemens, Lawrence Livermore Laboratory, Rept. UCRL-51577 (1974).

21. K.E. Apt and W.B. Walters, Phys. Rev. C 9, 310 (1974).

22. E.S. Macias and W.B. Walters, Nucl. Phys. A 160, 27[illegible] (1971).

23. S. Raman, R.L. Auble, and F.F. Dyer, Phys. Rev. C 9, 426 (1974).

24. R.L. Auble, J.B. Ball, and C.B. Fulmer, Phys. Rev. 169, 955 (1968).

25. G. Vanden Berghe and E. Degrieck, Z. Phys. 262, 25 (1973).

26. R.A. Meyer, Bull. Amer. Phys. Soc. 19, 501 (1974).

27. The experimentalist will note that a prime difficulty in identifying the population of the 1144-keV level for the first time is that the very intense 573-keV transition seems to produce a false peak in the gamma-ray spectra at approximately the same energy as the 1144.65-keV gamma ray. The final value resulted from use of absorbers, counting distance and differentiation of summing peaks and true photopeaks in the Compton Suppression Spectrometer spectra.

28. The experimental data comes from Refs. 26 and 29-32.

29. E. Booth, R. Arnold, and W. Alston, Phys. Rev. C 7, 1500 (1973).

30. P.D. Forsyth, quoted in Ref. 25.

31. P.C. Barnes, C. Ellegaard, B. Herskind, and M.C. Joshi, Phys. Lett. 23, 266 (1966).

32. D.J. Horen, Nucl. Data Sect. B 67, 75 (1971).

33. R. Auble, Ph.D. Thesis, Michigan State University, Lansing, Mich. (1968).

34. J.T. Larsen, R.G. Lanier, and R.A. Meyer, Bull. Amer. Phys. Soc. 18, 679 (1973).

35. R.G. Lanier, J.T. Larsen, and R.A. Meyer, Bull. Amer. Phys. Soc. 18, 679 (1973).

36. L.S. Kisslinger and R.A. Sorenson, Rev. Mod. Phys. 35, 853 (1963).

37. B.S. Reehal and R.A. Sorenson, Phys. Rev. C 2, 819 (1970).

38. C.E. Bemis and K. Fransson, Phys. Lett. 19, 567 (1965).

39. G. Alaga and G. Ialongo, Nucl. Phys. A 97, 600 (1965).

40. V. Paar, Phys. Lett. B 39, 466 (1972).

41. Ibid, p. 587.

42. R. Almar, O. Civitarese, and F. Krmpotic, Phys. Rev. C 8, 1518 (1973).

43. L.G. Mann, W.B. Walters, and R.A. Meyer, to be submitted to Phys. Rev. (1974).

44. D. Horen, Nucl. Data Sect. B 8, (2) 123 (1972).

45. B.W. Renwick, B. Byrne, D.A. Eastham, P.D. Forsyth, and D.G.E. Martin, Nucl. Phys. A 208, 574 (1973).

46. J. De Raedt, M. Rots, and H. Van de Voorde, Phys. Rev. C 9, 2391 (1974).

47. J. Kownacki, J. Ludziejewsky, and M. Moszynski, Nucl. Phys. A 107, 476 (1968).

48. W.B. Walters and R.A. Meyer, Bull. Amer. Phys. Soc. 17, 902 (1972).

49. L.G. Mann, W.B. Walters, and R.A. Meyer, Bull. Amer. Phys. Soc. 18, 1425 (1973).

50. R.L. Auble, J.B. Ball, and C.B. Fulmer, Phys. Rev. 169, 955 (1968).

51. G. Vanden Berghe, Z. Phys. 266, 266 (1974).

52. A. Kerek, P. Carle, and S. Borg, Nucl. Phys. A 224, 367 (1974).

53. L.V. Peker, Multiparticle States, Winter School for Nuclear Theory and High Energy Physics (1969), Lawrence Livermore Laboratory, UCRL-Trans. 1399.

54. S.V. Jackson, W.B. Walters, and R.A. Meyer, submitted to Phys. Rev. C (1974).

55. W.B. Walters, S.V. Jackson, and R.A. Meyer, in Proc. Topical Conf. Vibrational Nuclei, Zagreb, Yugoslavia, 1974.

56. R.A. Meyer, J.H. Landrum, and S.C. Bourret, Spectroscopy Investigation of the Fission Precursors of ^{131,133,135}Xe, Lawrence Livermore Laboratory, Final Rept., 1974 (in preparation).

57. J.R. Leigh, K. Nakai, K.H. Maier, F. Puhlhofer, F.S. Stephens, and R.M. Diamond, Nucl. Phys. A 213, 1 (1973).

58. F.S. Stephens, R.M. Diamond, and S.G. Nilsson, Phys. Lett. B 44, 429 (1973).

59. K. Nakai, P. Kleinheinz, J.R. Leigh, K.H. Maier, F.S. Stephens, R.M. Diamond, and G.L. Løvhøiden, Phys. Lett. B 44, 443 (1973).

60. F.S. Stephens, R.M. Diamond, J.R. Leigh, T. Kammuri, and K. Nakai, Phys. Rev. Lett. 29, 438 (1972).

61. E.A. Henry and R.A. Meyer, Bull. Amer. Phys. Soc. 19, 502 (1974).

62. E.A. Henry and R.A. Meyer, Z. Phys. (1974) (in press).

63. E.A. Henry, C. Gatrousis, and R.A. Meyer, Bull. Amer. Phys. Soc. 18, 680 (1973).

64. J. Meyer ter Vehn, Lawrence Berkeley Laboratory, private communication (April 1974).

65. See, e.g., M. Sakai, Nucl. Data Tables 10, 511 (1972), and J.F. Wild and R.A. Meyer, in Proc. Am. Chem. Soc. Meeting, Los Angeles, 1974.

66. J.R. Comfort and K.R.S. Devan, Bull. Amer. Phys. Soc. 19, 61 (1974); private communication (April 1974).

67. F.S. Dietrich et al., Nucl. Phys. A 155, 209 (1970).

68. J. McDonald, D. Parter, and D.T. Stewart, Nucl. Phys. A 104, 177 (1967).

69. G. Graffee, C.W. Tang, C.D. Coryell, and G.E. Gordon, Phys. Rev. 149, 884 (1966).

70. A. Bäcklin, B. Fogelberg, and S.G. Malinskog, Nucl. Phys. A 96, 539 (1967).

71. R.A. Meyer and G.L. Struble, J. Phys. Soc. Japan, 34, 418 (1973).

72. R.A. Meyer, J.T. Larsen, and R.G. Lanier, in Proc. Intern. Conf. Nucl Phys., Munich, 1973.

73. J. Brownlee and R.A. Meyer, Bull. Amer. Phys. Soc. 18, 703 (1973).

74. A.A. Delucchi and R.A. Meyer, Bull. Amer. Phys. Soc. 18, 703 (1973).

75. N. Smith and R.A. Meyer, Bull. Amer. Phys. Soc. 17, 586 (1972).

76. S.V. Jackson, W.B. Walters, and R.A. Meyer, to be published (1974).

77. E.S. Macias, R.E. Head, H.C. Hseuh, and M.R. Zalutsky, Nucl. Instr. Methods to be published (1974).

78. H.J. Kim and R.L. Robinson, Phys. Rev. C 9, 767 (1974).

79. A. Bäcklin, Institute for Nuclear Physics, Stockholm, private communication (1974).

80. E.M. Bernstein, G.G. Seamon, and J.M. Palms, Nucl. Phys. A 141, 67 (1970).

81. A. Marcinkowski, A. Bäcklin, and I. Bergquist, Nucl. Phys. 179, 781 (1972).

82. E.V. Weiffenbach and R. Tickle, Phys. Rev. C 3, 1668 (1971).

83. M. Conjeaud, S. Harar, and E. Thuriere, Nucl. Phys. A 129, 10 (1969).

84. W.H. Hasselink, B.R. Kooistra, L.W. Put, R.H. Siemssen, and S. van der Werf, Nucl. Phys. A 226, 209 (1974).

85. M. Conjeaud, S. Harar, and E. Thuriere, Commissariat a l'Energie Atomique, Rept. CEA-N-1232 (1969), p. 36.

86. H. Haas and P.A. Shirley, Lawrence Berkeley Laboratory, Rept. UCRL-20426 (1970).

87. A. Covello, V.R. Manfredi, and N. Azziz, Nucl. Phys. A 201, 215 (1973).

88. B.I. Atalay and L.W. Chiao-Yap, Phys. Rev. C 5, 369 (1972).

89. S. Sen, Nucl. Phys. A 191, 29 (1972).

90. M.J. Mang, F. Krmpotic, and S.M. Abecasis, Z. Phys. 262, 39 (1973).

91. R.K. Jolly and E. Kashy, Phys. Rev. C 4, 1398 (1971).

92. A. Chaumeaux, G. Brugge, H. Faraggi, and J. Picard, Nucl. Phys. A 164, 176 (1971).

93. E.S. Macias, J.P. OpDeBeech, and W.B. Walters, Nucl. Phys. A 147, 513 (1970).

94. J.D. King, N. Neff, and H.W. Taylor, Nucl. Phys. A 99, 433 (1967).

95. D.B. Berry, W.H. Kelly, and W.C. McHarris, Phys. Rev. 188, 1875 (1969).

96. M. Zalutsky, E.S. Macias, and R.A. Meyer, to be published (1974).

97. R.A. Meyer, J.H. Landrum, and W.B. Walters, to be published (1974).

98. R.A. Meyer, J.H. Landrum, and J.T. Larsen, to be published (1974).

99. C.M. Lederer, Lawrence Berkeley Laboratory, private communication (1974).

100. K. Heyde and P.J. Brussaard, Z. Phys. 259, 15 (1973).

101. K. Heyde and P.J. Brussaard, Nucl. Phys. A 104, 81 (1967).

102. K. Heyde and P.J. Brussaard, Nucl. Phys. A 112, 494 (1968).

103. H. Vanden Berghe and K. Heyde, Nucl. Phys. A 163, 478 (1970).

104. S. Sen, P.J. Riley, and T. Udagawa, Phys. Rev. C 6, 2201 (1972).

105. R. Bunting, Nucl. Data Sect. B, to be published, and private communication (1974).

106. A. Kerek, J. Kownacki, A. Marelins, and J. Pihl, Nucl. Phys. A 194, 64 (1972).

107. D. Kurath and R.D. Lawson, Phys. Rev. 161, 915 (1967).

108. R.A. Meyer and W.B. Walters, to be submitted to Phys. Rev. (1974).

109. R.L. Auble, Nucl. Data Sect. B 7, 465 (1972).

110. See, e.g., Refs. 100 and 101.

111. I am indebted to C.M. Lederer of Lawrence Berkeley Laboratory and his staff for making available to me the data in their forthcoming compilation of nuclear data (Table of Isotopes, 7th Ed.).

112. See, e.g., J.D. Immele and G.L. Struble, Phys. Rev. C 9, 460 (1974).

FIGURE CAPTIONS

Fig. 1. Systematics of odd-mass antimony nuclei. Insert shows trend of lowest levels with respect to the $g_{7/2}$ state.

Fig. 2. Decay schemes of ^{121}Te (top) and ^{113}Sn (bottom).

Fig. 3. Decay of the $1/2^-$ and $3/2^-$ levels in ^{119}Sb populated in the decay of ^{119}Te. (N.B. The first number in parentheses represents the gamma-ray branching in the ^{119}Te decay; the second number represents the relative hindrance from a single-particle estimate.)

Fig. 4. Comparison of ^{129}I levels observed in experiments (center) with those predicted by three-particle calculations of Almar et al. (left) and Vanden Berghe (right).

Fig. 5. Decay properties of selected levels in ^{131}I (left) and ^{133}I (right) and comparison of their observed negative-parity levels (center).

Fig. 6. Levels of ^{133}I to 2 MeV populated in the decay of ^{133}Te^m. (N.B. Dots below an arrow indicate that the placement of that gamma ray has been confirmed by gamma-gamma coincidence experiments; see Appendix I.)

Fig. 7. Systematics of lowest levels in odd-mass lanthanum nuclei (bottom). Decay of selected levels of ^{133}La (top right). Comparison of levels of ^{133}La obtained by experiment and calculation (top left): (A) particle, (B) with pairing (see text).

Fig. 8. Systematics of odd-mass nuclei with 81 neutrons.

Fig. 9. Decay of ^{135}Xe levels up to 2 MeV (bottom). Comparison of ^{135}Xe levels observed in experiment with those expected from coupling a $s_{1/2}$ or $d_{3/2}$ hole and the known ^{136}Xe core (top).

Fig. 10. Decay of selected levels in ^{133}Te populated in the decay of 2.45-*min* ^{133}Sb.

Fig. 11. Current status of various nuclear models (see text).

JKP/md

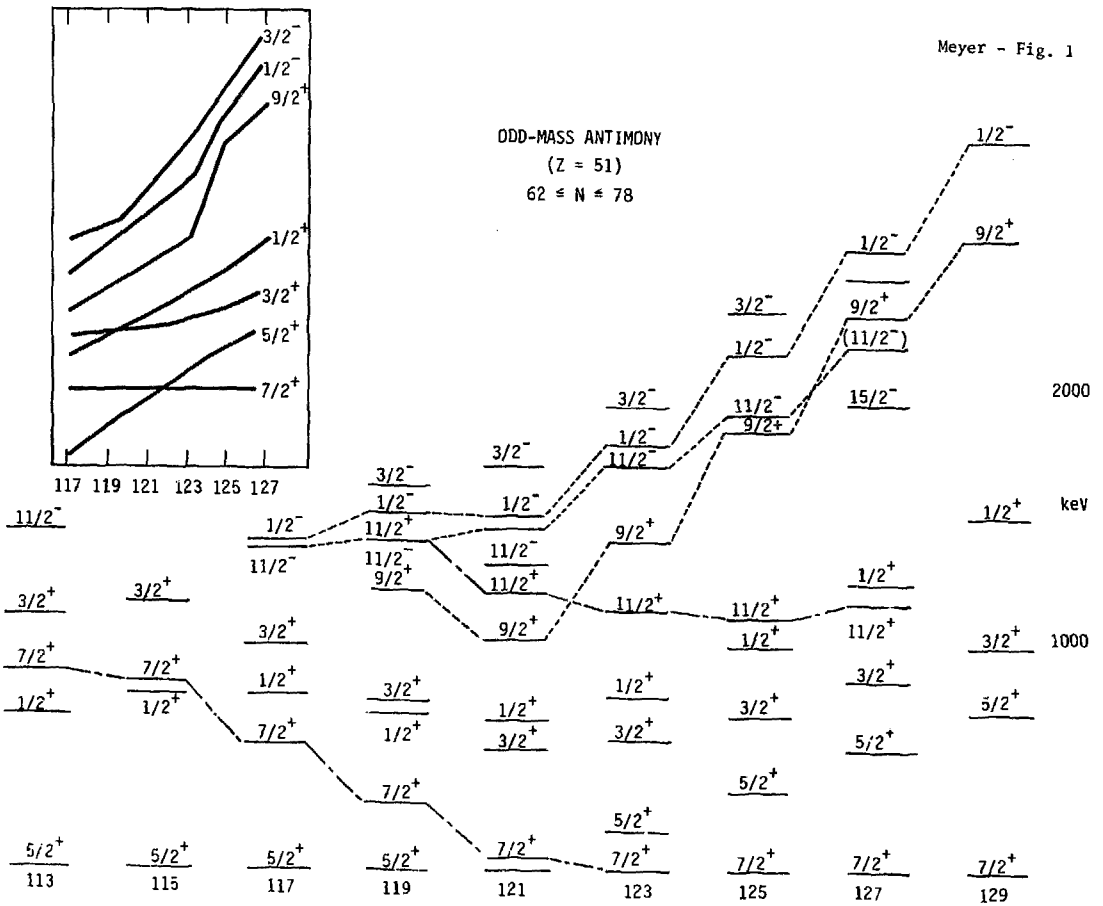
Meyer - Fig. 1
ODD-MASS ANTIMONY
(Z = 51)
62 ≤ N ≤ 78
3/2⁻
1/2⁻
9/2⁺
1/2⁺
3/2⁺
5/2⁺
7/2⁺
117 119 121 123 125 127
2000
1000
keV
11/2⁻
3/2⁺
7/2⁺
1/2⁺
5/2⁺
113
115
117
119
121
123
125
127
129
(11/2⁻)
15/2⁻
9/2+
11/2⁺

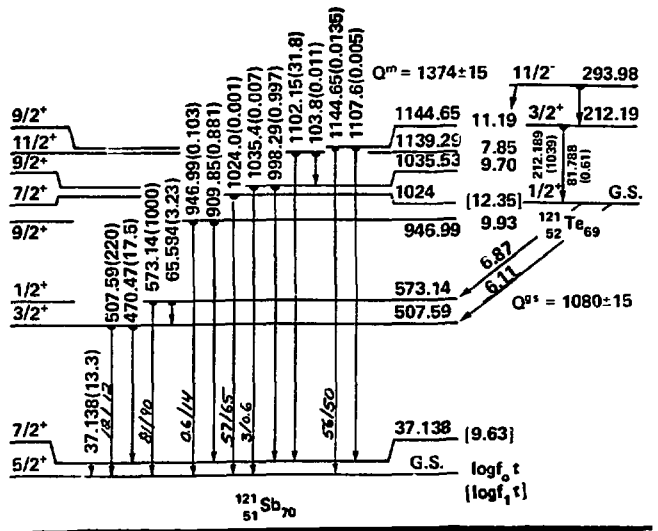
Q^m = 1374±15
11/2⁻ 293.98
3/2⁺ 212.19
1/2⁺ G.S.
121 52 Te 69
Q^gs = 1080±15
1144.65
1139.29
1035.53
1024
946.99
573.14
507.59
37.138 [9.63]
G.S.
logf₀t
[logf₁t]
121 51 Sb 70

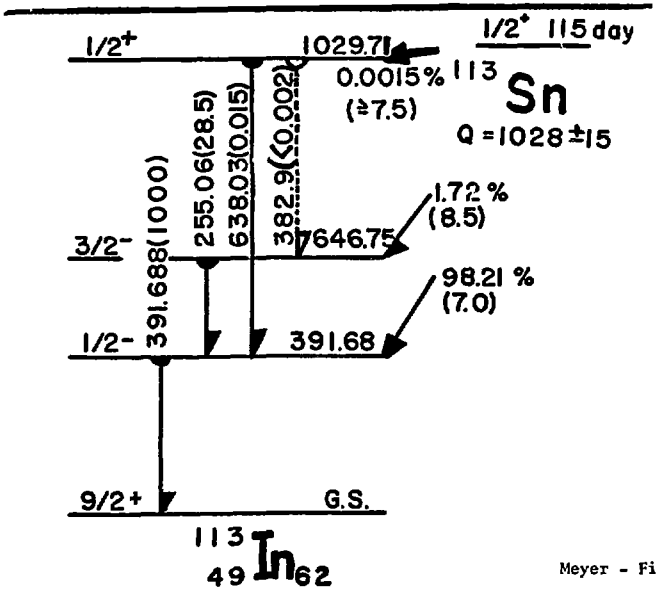
1/2⁺ 115 day
1029.71
0.0015% 113 Sn
(≥7.5)
Q = 1028±15
1.72 %
(8.5)
7646.75
98.21 %
(7.0)
391.68
G.S.
113 49 In 62

Meyer - Fig. 2

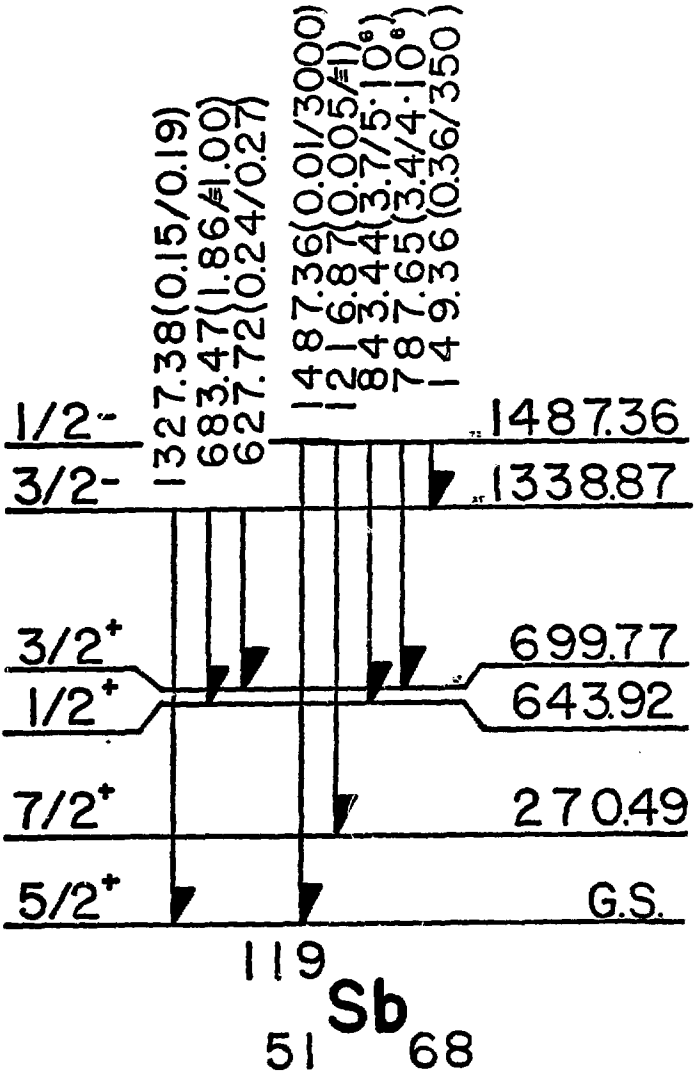
1327.38(0.15/0.19)
683.47(1.86/1.00)
627.72(0.24/0.27)
1487.36(0.01/3000)
1216.87(0.005/1)
843.44(3.7/5·10⁶)
787.65(3.4/4·10⁶)
149.36(0.36/350)
1/2⁻
1487.36
3/2⁻
1338.87
3/2⁺
699.77
1/2⁺
643.92
7/2⁺
270.49
5/2⁺
G.S.
119
51 Sb 68

Meyer - Fig. 3

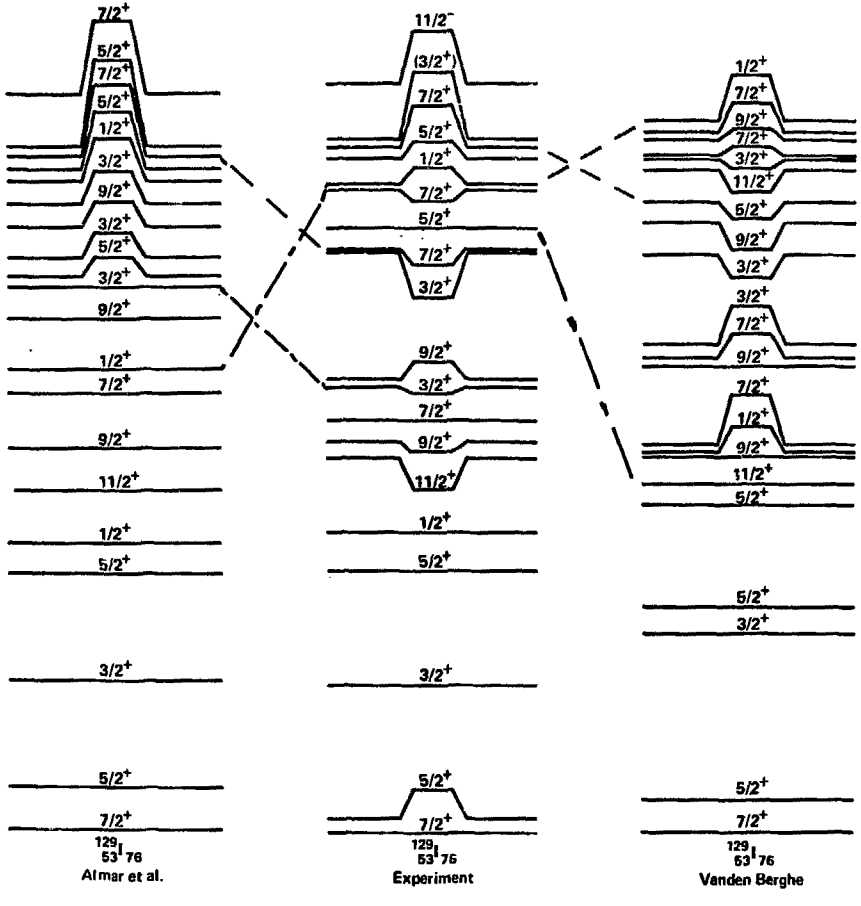
7/2+
5/2+
7/2+
5/2+
1/2+
3/2+
9/2+
3/2+
5/2+
3/2+
9/2+
1/2+
7/2+
9/2+
11/2+
1/2+
5/2+
3/2+
5/2+
7/2+
129 53 I 76
Almar et al.
11/2-
(3/2+)
7/2+
5/2+
1/2+
7/2+
5/2+
7/2+
3/2+
9/2+
3/2+
7/2+
9/2+
11/2+
1/2+
5/2+
3/2+
5/2+
7/2+
129 53 I 76
Experiment
1/2+
7/2+
9/2+
7/2+
3/2+
11/2+
5/2+
9/2+
3/2+
3/2+
7/2+
9/2+
7/2+
1/2+
9/2+
11/2+
5/2+
5/2+
3/2+
5/2+
7/2+
129 53 I 76
Vanden Berghe

Meyer - Fig. 4

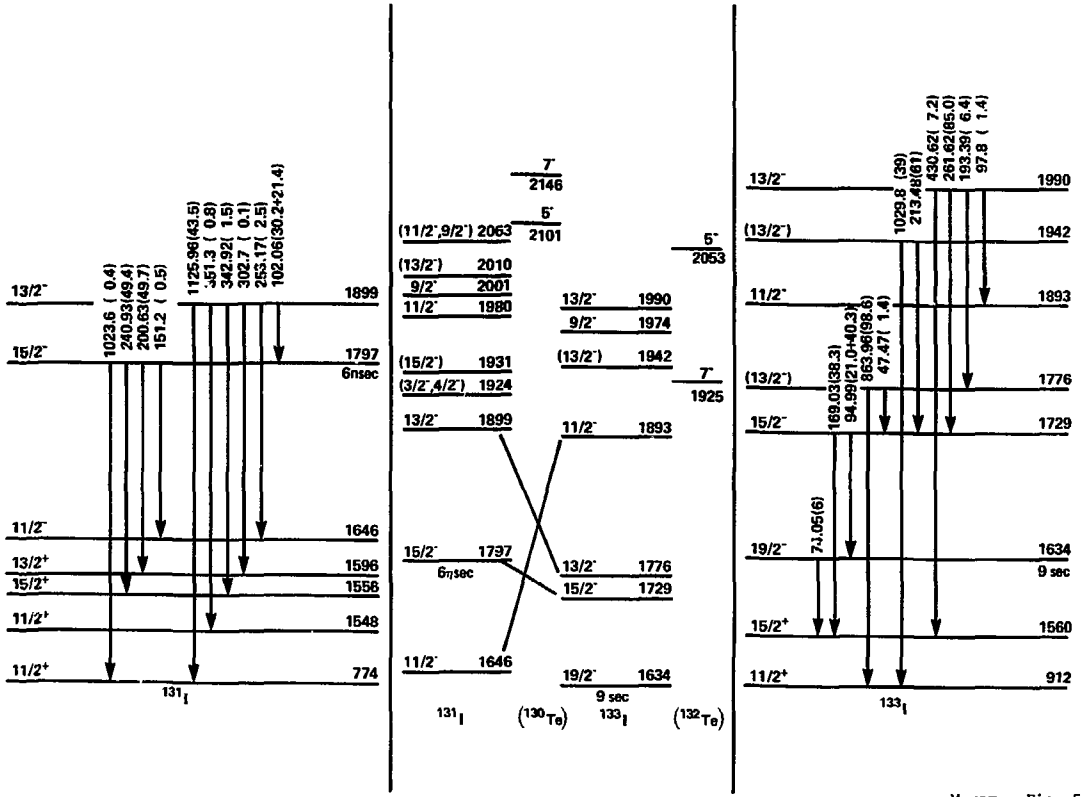
13/2⁻ 1899
15/2⁻ 1797
6nsec
11/2⁻ 1646
13/2⁺ 1596
15/2⁺ 1556
11/2⁺ 1548
11/2⁺ 774
131I
1023.6 (0.4)
240.93(49.4)
200.63(49.7)
151.2 (0.5)
1125.96(43.5)
351.3 (0.8)
342.92(1.5)
302.7 (0.1)
253.17(2.5)
102.06(30.2+21.4)
7⁻ 2146
5⁻ 2101
(11/2⁻,9/2⁻) 2063
(13/2⁻) 2010
9/2⁻ 2001
11/2⁻ 1980
(15/2⁻) 1931
(3/2⁻,4/2⁻) 1924
13/2⁻ 1899
15/2⁻ 1797
6η sec
11/2⁻ 1646
131I
(130Te)
13/2⁻ 1990
9/2⁻ 1974
(13/2⁻) 1942
11/2⁻ 1893
13/2⁻ 1776
15/2⁻ 1729
19/2⁻ 1634
9 sec
133I
(132Te)
5⁻ 2053
7⁻ 1925
13/2⁻ 1990
(13/2⁻) 1942
11/2⁻ 1893
(13/2⁻) 1776
15/2⁻ 1729
19/2⁻ 1634
9 sec
15/2⁺ 1560
11/2⁺ 912
133I
1029.8 (39)
213.48(61)
430.62(7.2)
261.62(85.0)
193.39(6.4)
97.8 (1.4)
169.03(38.3)
94.99(21.0+40.3)
863.96(98.6)
47.47(1.4)
74.05(6)

Meyer - Fig. 5

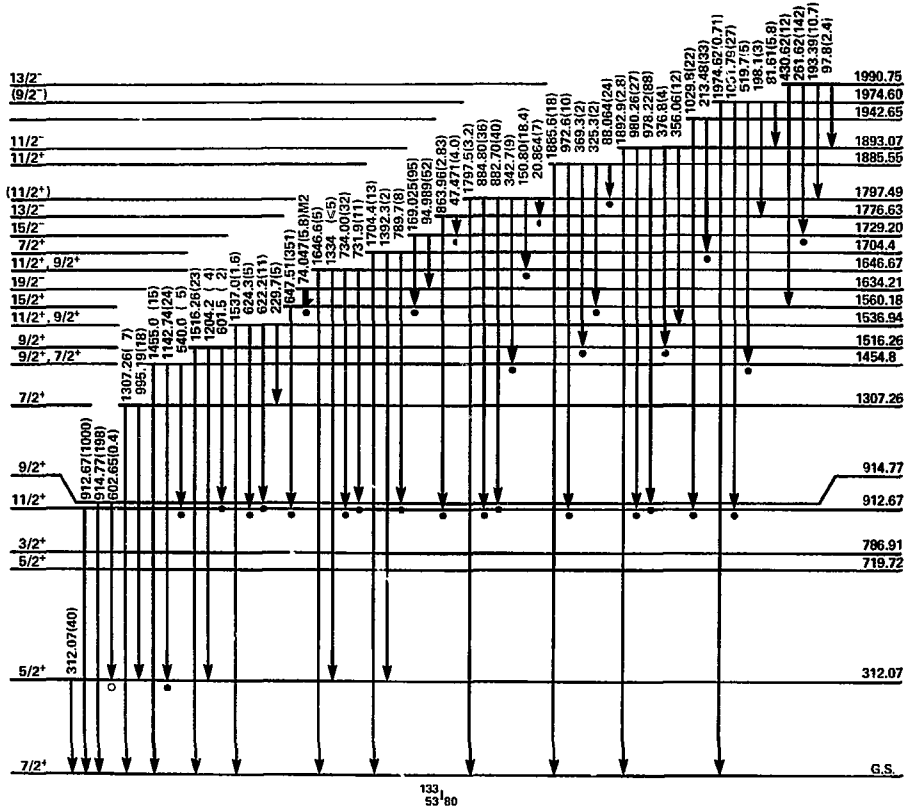
13/2⁻
(9/2⁻)
11/2⁻
11/2⁺
(11/2⁺)
13/2⁻
15/2⁻
7/2⁺
11/2⁺, 9/2⁺
19/2⁻
15/2⁺
11/2⁺, 9/2⁺
9/2⁺
9/2⁺, 7/2⁺
7/2⁺
9/2⁺
11/2⁺
3/2⁺
5/2⁺
5/2⁺
7/2⁺
1990.75
1974.60
1942.65
1893.07
1885.55
1797.49
1776.63
1729.20
1704.4
1646.67
1634.21
1560.18
1536.94
1516.26
1454.8
1307.26
914.77
912.67
786.91
719.72
312.07
G.S.
312.07(40)
912.67(1000)
914.77(198)
602.65(0.4)
1307.26(7)
995.1(18)
914.77(198)
1465.0 (15)
1142.74(24)
640.01 (5)
1616.26(23)
1204.2 (4)
601.5 (2)
1537.0(1.6)
624.3(5)
622.2(11)
229.7(5)
1647.51(351)
74.047(5.8)M2
1646.6(5)
1334 (<5)
734.00(32)
731.9(11)
1704.4(13)
1392.3(2)
789.7(8)
169.025(95)
94.989(52)
863.96(2.83)
47.471(4.0)
1797.5(3.2)
884.80(36)
882.70(40)
342.7(9)
150.80(16.4)
20.864(7)
1885.6(18)
972.6(10)
369.3(2)
325.3(2)
88.064(24)
1892.9(2.8)
980.26(27)
978.22(88)
376.8(4)
356.06(12)
1029.8(22)
213.48(33)
1974.62(0.71)
1051.79(27)
519.7(5)
198.1(3)
511.6(15.8)
430.62(12)
281.62(142)
193.39(10.7)
97.8(2.4)
133 53 80 I

Meyer - Fig. 6

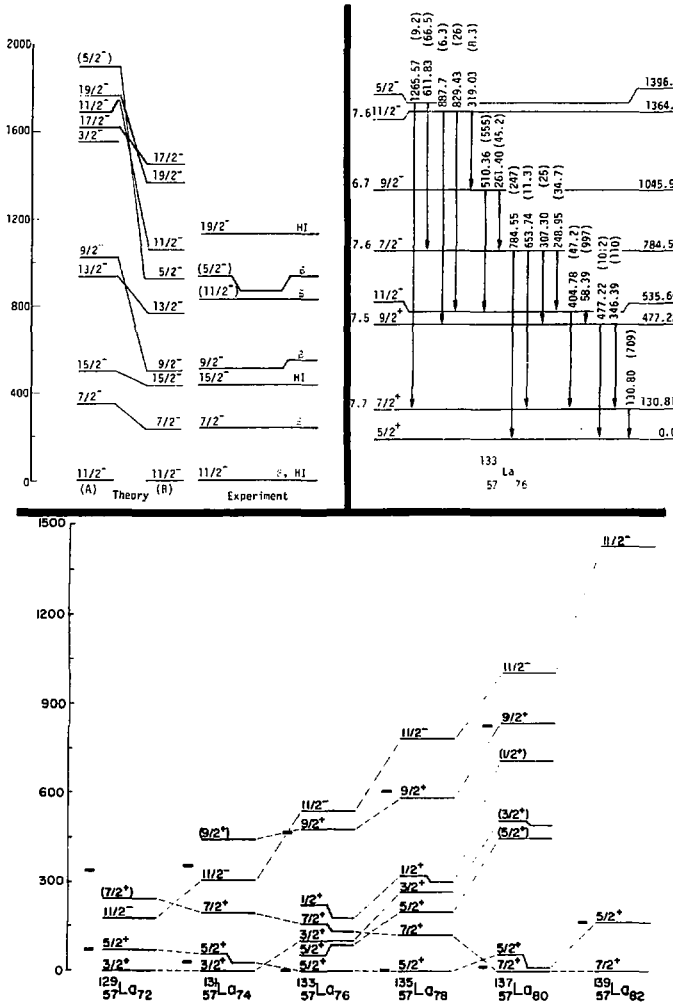
2000
1600
1200
800
400
0
(5/2⁻)
19/2⁻
11/2⁻
17/2⁻
3/2⁻
17/2⁻
19/2⁺
11/2⁻
9/2⁻
13/2⁻
5/2⁻
13/2⁻
15/2⁻
9/2⁻
15/2⁻
7/2⁻
7/2⁻
11/2⁻ (A)
11/2⁻ (B)
Theory
19/2⁻ HI
(5/2⁻)
(11/2⁻)
9/2⁻
15/2⁻ HI
7/2⁻
11/2⁻ 8, HI
Experiment
(9.2)
(66.5)
(6.3)
(26)
(n.3)
1265.57
611.83
887.7
829.43
319.03
5/2⁻
7.6 11/2⁻
6.7 9/2⁻
7.6 7/2⁻
11/2⁻
7.5 9/2⁺
7.7 7/2⁺
5/2⁺
1396.5
1364.9
1045.95
784.54
535.60
477.22
130.81
0.0
510.36 (555)
261.40 (45.2)
784.55 (247)
653.74 (11.3)
307.30 (25)
240.95 (34.7)
404.78 (47.2)
58.39 (997)
477.22 (10.2)
346.39 (110)
130.80 (709)
133 La 57 76
1500
1200
900
600
300
0
11/2⁻
9/2⁺
(1/2⁺)
(3/2⁺)
(5/2⁺)
(9/2⁺)
(7/2⁺)
1/2⁺
3/2⁺
5/2⁺
7/2⁺
129 57La72
131 57La74
133 57La76
135 57La78
137 57La80
139 57La82

Meyer - Fig. 7

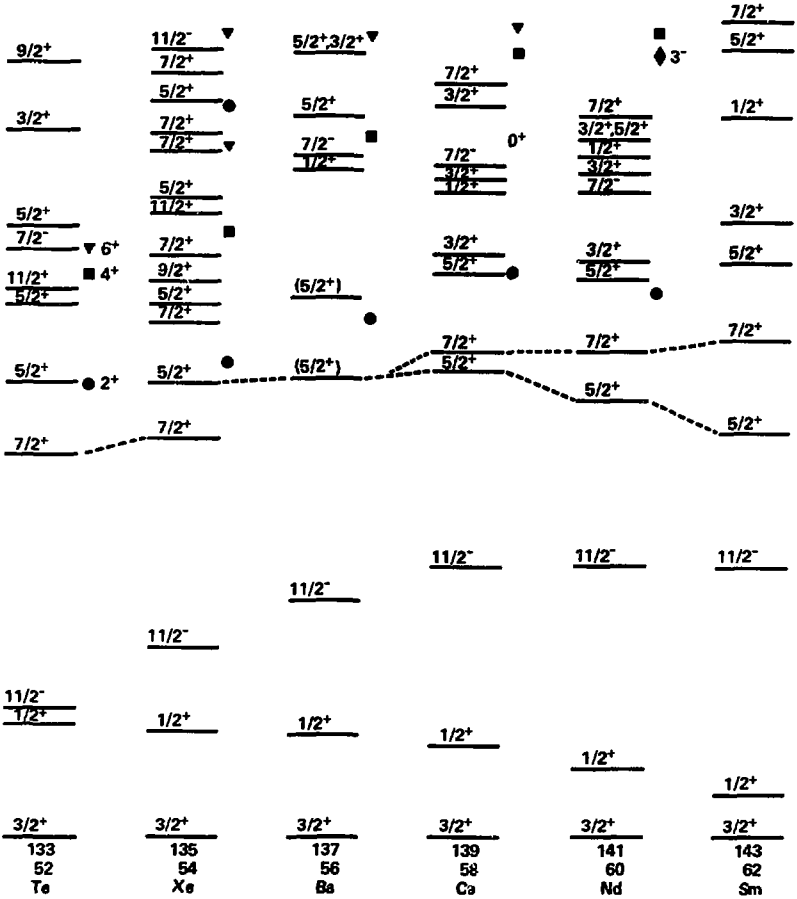
9/2+
3/2+
5/2+
7/2-
6+
11/2+
4+
5/2+
5/2+
2+
7/2+
11/2-
7/2+
5/2+
7/2+
7/2+
5/2+
11/2+
7/2+
9/2+
5/2+
7/2+
5/2+
7/2+
5/2+,3/2+
5/2+
7/2-
1/2+
(5/2+)
(5/2+)
7/2+
3/2+
7/2+
3/2+
0+
7/2-
3/2+
1/2+
3/2+
5/2+
7/2+
5/2+
3-
7/2+
3/2+,5/2+
1/2+
3/2+
7/2-
3/2+
5/2+
7/2+
5/2+
7/2+
1/2+
3/2+
5/2+
7/2+
5/2+
11/2-
1/2+
3/2+
133
52
Te
11/2-
1/2+
3/2+
135
54
Xe
11/2-
1/2+
3/2+
137
56
Ba
11/2-
1/2+
3/2+
139
58
Ce
11/2-
1/2+
3/2+
141
60
Nd
11/2-
1/2+
3/2+
143
62
Sm

Meyer - Fig. 8

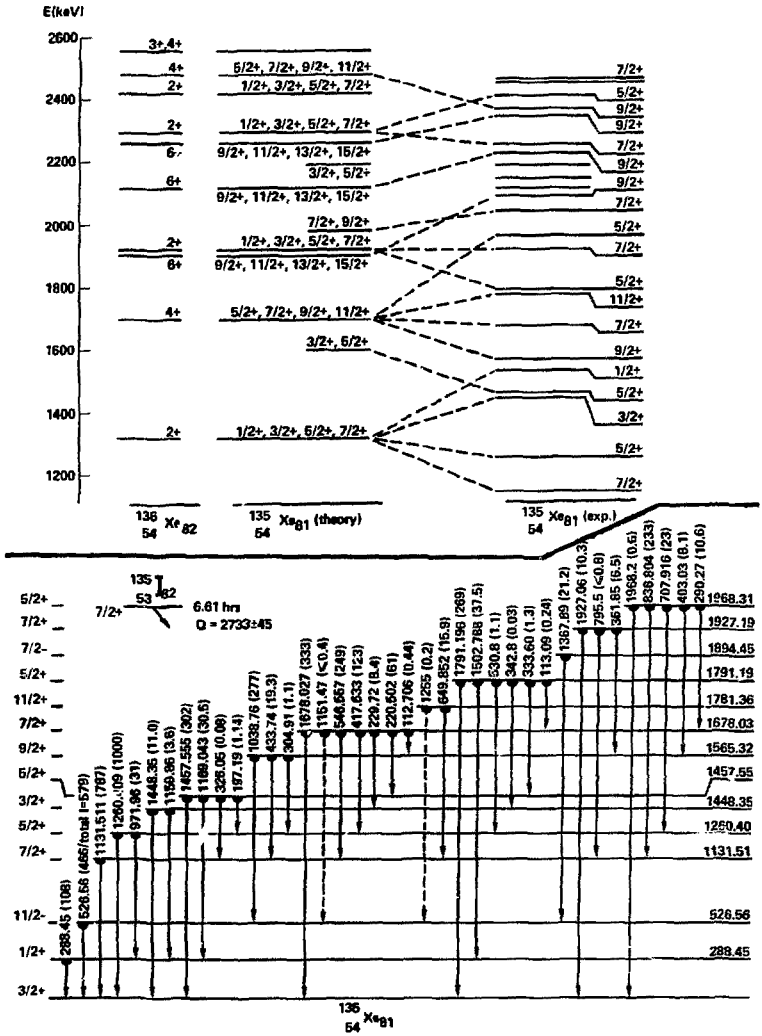
E(keV)
2600
2400
2200
2000
1800
1600
1400
1200
3+,4+
4+
2+
2+
6-
6+
2+
6+
4+
2+
5/2+, 7/2+, 9/2+, 11/2+
1/2+, 3/2+, 5/2+, 7/2+
1/2+, 3/2+, 5/2+, 7/2+
9/2+, 11/2+, 13/2+, 15/2+
3/2+, 5/2+
9/2+, 11/2+, 13/2+, 15/2+
7/2+, 9/2+
1/2+, 3/2+, 5/2+, 7/2+
9/2+, 11/2+, 13/2+, 15/2+
5/2+, 7/2+, 9/2+, 11/2+
3/2+, 5/2+
1/2+, 3/2+, 5/2+, 7/2+
7/2+
5/2+
9/2+
9/2+
7/2+
9/2+
9/2+
7/2+
5/2+
7/2+
5/2+
11/2+
7/2+
9/2+
1/2+
5/2+
3/2+
5/2+
7/2+
136 54 Xe 82
135 54 Xe 81 (theory)
135 54 Xe 81 (exp.)
135 53 82
7/2+
6.61 hrs
Q = 2733±45
5/2+
7/2+
7/2-
5/2+
11/2+
7/2+
9/2+
5/2+
3/2+
5/2+
7/2+
11/2-
1/2+
3/2+
288.45 (106)
526.56 (455/total I=579)
1131.511 (787)
1260.409 (1000)
971.96 (31)
1448.35 (11.0)
1159.86 (3.6)
1457.555 (302)
1189.043 (30.5)
326.05 (0.06)
197.19 (1.14)
1038.76 (277)
433.74 (19.3)
304.91 (1.1)
1678.027 (333)
1151.47 (<0.4)
546.557 (249)
417.533 (123)
229.72 (8.4)
220.502 (61)
112.706 (0.44)
1255 (0.2)
649.852 (15.9)
1791.196 (269)
1502.788 (37.5)
530.8 (1.1)
342.8 (0.03)
333.60 (1.3)
113.09 (0.24)
1367.89 (21.2)
1927.06 (10.3)
795.5 (<0.8)
361.85 (6.5)
1968.2 (0.6)
838.804 (233)
707.916 (23)
493.03 (8.1)
290.27 (10.6)
1968.31
1927.19
1894.45
1791.19
1781.36
1678.03
1565.32
1457.55
1448.35
1260.40
1131.51
526.56
288.45
136 54 Xe 81

Meyer - Fig. 9

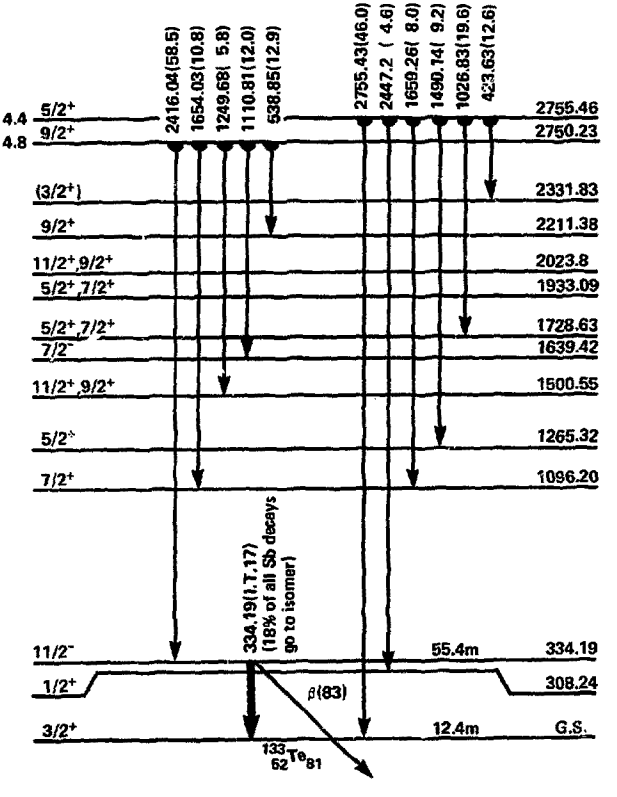
2416.04(58.5)
1654.03(10.8)
1249.68(5.8)
1110.81(12.0)
538.85(12.9)
2755.43(46.0)
2447.2 (4.6)
1659.26(8.0)
1490.14(9.2)
1026.83(19.6)
423.63(12.6)
4.4 5/2+
4.8 9/2+
2755.46
2750.23
(3/2+)
2331.83
9/2+
2211.38
11/2+,9/2+
2023.8
5/2+,7/2+
1933.09
5/2+,7/2+
1728.63
7/2-
1639.42
11/2+,9/2+
1500.55
5/2+
1265.32
7/2+
1096.20
334.19(1.7,17)
(18% of all Sb decays
go to isomer)
11/2-
55.4m
334.19
1/2+
308.24
β(83)
3/2+
12.4m
G.S.
133 52Te81

Meyer - Fig. 10

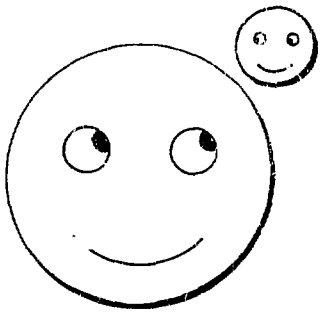

SINGLE PARTICLE

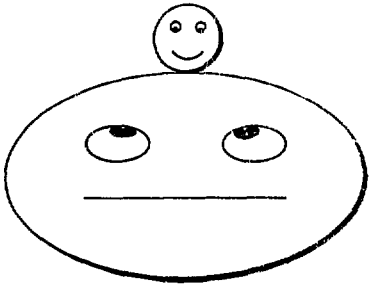

VIBRATION COUPLED

ROTATION ALIGNED

Meyer - Fig. 11